Research paper

Complex Formation Reactions of Gallium(III) and Iron(III/II) with L-Proline-Thiosemicarbazone Hybrids: a Comparative Study

Felix Bacher, Orsolya Dömötör, Éva A. Enyedy, Lana Filipović, Siniša Radulović, Gregory S. Smith, Vladimir B. Arion

PII: S0020-1693(16)30357-7
DOI: http://dx.doi.org/10.1016/j.ica.2016.06.044
Reference: ICA 17135

To appear in: *Inorganica Chimica Acta*

Received Date: 12 February 2016
Revised Date: 28 June 2016
Accepted Date: 29 June 2016

Please cite this article as: F. Bacher, O. Dömötör, E.A. Enyedy, L. Filipović, S. Radulović, G.S. Smith, V.B. Arion, Complex Formation Reactions of Gallium(III) and Iron(III/II) with L-Proline-Thiosemicarbazone Hybrids: a Comparative Study, *Inorganica Chimica Acta* (2016), doi: http://dx.doi.org/10.1016/j.ica.2016.06.044

Complex Formation Reactions of Gallium(III) and Iron(III/II) with L-Proline-Thiosemicarbazone Hybrids: a Comparative Study

Felix Bacher[a], Orsolya Dömötör[b,c], Éva A. Enyedy[b]✉, Lana Filipović[d], Siniša Radulović[d], Gregory S. Smith[e], Vladimir B. Arion[a]✉

[a]Institute of Inorganic Chemistry, University of Vienna, Währinger Strasse 42, 1090 Vienna, Austria; [b]Department of Inorganic and Analytical Chemistry, University of Szeged, Dóm tér 7, H-6720 Szeged, Hungary; [c] MTA-SZTE Bioinorganic Chemistry Research Group, University of Szeged, Dóm tér 7, H-6720 Szeged, Hungary; [d]Institute for Oncology and Radiology of Serbia, Pasterova 14, 11000 Belgrade, Serbia; [e]Department of Chemistry, University of Cape Town, Rondebosch, 7701, Cape Town, South Africa

felix.bacher@univie.ac.at, domotor.o@chem.u-szeged.hu, enyedy@chem.u-szeged.hu, lanafil82@gmail.com, sinisar@ncrc.ac.rs, gregory.smith@uct.ac.za, vladimir.arion@univie.ac.at
✉ enyedy@chem.u-szeged.hu, Department of Inorganic and Analytical Chemistry, University of Szeged, Dóm tér 7, H-6720 Szeged, Hungary

✉ vladimir.arion@univie.ac.at, Institute of Inorganic Chemistry, University of Vienna, Währinger Strasse 42, 1090 Vienna, Austria, tel: +43 1 4277 52615, fax: +43 1 4277 52630

Abstract

Three novel gallium(III) and iron(III) complexes with L-proline-thiosemicarbazone hybrids, namely [GaCl(L-Pro-FTSC–2H)]·0.7H_2O·0.5CH_3OH (**1**·0.7H_2O·0.5CH_3OH), [GaCl(dm-L-Pro-FTSC–2H)]·0.4H_2O (**2**·0.4H_2O) and [FeCl(L-Pro-FTDA–H)]Cl (**3**) were synthesised and comprehensively characterised by spectroscopic methods (^{1}H, ^{13}C NMR, UV−vis), ESI mass spectrometry and X-ray crystallography. The complexes are soluble in biological media to allow for assaying their antiproliferative activity. The complexes were tested in three human cancer cell lines, namely HeLa, A549 (non-small cell lung cancer), LS174 and nontumorigenic MRC5. Complex formation equilibrium processes of L-Pro-FTSC with gallium(III), iron(II) and iron(II) ions were investigated in solution. The formation of mono-ligand iron(II) and gallium(III) complexes with pentadentate ligands and relatively low aqueous solution stability was found. Between iron(III) and the ligands, a redox reaction takes place via the oxidative cyclisation of the thiosemicarbazones.

Keywords: Thiosemicarbazones, Gallium(III), Iron(III), Antiproliferative activity

1. Introduction

Gallium(III) is the second metal ion after platinum(II) which is applied in anticancer therapy. Gallium(III) nitrate showed anticancer activity in bladder cancer and non-Hodgkin's lymphoma in clinical trials[1,2,3,4,5] and is currently approved for the treatment of cancer related hypercalcemia.[6] Gallium(III) strongly resembles iron(III) as both ions have comparable ionic radii. In fact, this also explains the biological activities of gallium(III): it is believed that the human body cannot distinguish between iron(III) and gallium(III), therefore both use the same transport pathways and are bound to the same proteins, with the difference that gallium(III) is virtually irreducible under physiological conditions.[7] Many malignancies and in general, fast dividing tissues have an enhanced demand for iron, which leads to a characteristic overexpression of transferrin receptors on the cell surface in many cancer types.[8,9,10] Consequently gallium(III), which is almost exclusively bound to transferrin in the human blood plasma,[11] accumulates in many cancers to a greater amount than in normal tissues. ^{67}Ga is therefore suitable for tumor detection.[12]

Iron is necessary for the synthesis of ribonucleotide reductase (RNR), an enzyme that performs the rate determining step of DNA synthesis, namely, the reduction of ribonucleotides to the corresponding deoxyribonucleotides. It contains a diferric tyrosyl radical cofactor which is essential for its function.[13,14] It is known that gallium(III) is able to replace the iron(III) ions in RNR and thereby inhibits its activity.[15] A problem in the use of simple gallium salts, such as gallium(III) nitrate for cancer treatment is their fast hydrolysis in the human blood stream, leading to the precipitation of sparingly soluble gallium(III) hydroxides and consequently a low bioavailability.[7,16] This led to the development of more stable gallium complexes, namely gallium(III) maltolate, tris(3-hydroxy-2-methyl-4*H*-pyran-4-onato)gallium(III) and tris(8-quinolinolato)gallium(III) (KP46) which are currently under clinical investigation.[17] Gallium complexes with thiosemicarbazone and thiocarbohydrazone ligands are also of interest for anticancer therapy.[18] Thiosemicarbazones (TSCs) are potent metal chelators with a broad spectrum of biological activity.[19,20,21,22,23,24] Tibione or *p*-acetylaminobenzaldehyde TSC was used as a drug against tuberculosis.[25] Their anticancer activity was discovered in the 1960s when 2-formylpyridine TSC was tested in a leukemia bearing mouse model.[26] The best studied TSC to date is 3-aminopyridine-2-carboxaldehyde TSC or Triapine, which was evaluated in several

clinical phase I and II trials. Overall, Triapine is inactive against solid tumors but shows promising results against leukemia and other blood malignancies.[27,28,29,30,31,32,33,34,35,36] TSCs are inhibitors of the enzymes RNR and Topoisomerase IIα, both of which are good targets for anticancer therapy, since they are essential for cell division.[14,37,38,39,40,41,42] Metal complexation plays an important role in the activity of TSCs. In the case of Triapine and related RNR inhibiting TSCs, for example, it is not the free ligand precursors but their *in vivo* formed iron(II) complex that is the active species. The iron(II) bis(Triapine) complex is able to reduce a diferric tyrosyl radical in the R2 subunit of RNR, which quenches the enzyme activity.[43,44,45,46] On the other hand copper(II) complexation of Topoisomerase IIα inhibiting TSCs, leading to square-planar complexes, enhances their activity markedly.[47] A possible synergistic effect in RNR inhibition is the rationale for the synthesis of gallium(III)-TSC complexes. An increased cytotoxicity of gallium(III)-TSC complexes has been observed when compared to the free ligands (ligand precursors) and the corresponding iron(III)-TSC complexes, although the iron(III)-TSC complexes quenched the RNRs tyrosyl radical faster than its gallium(III) counterparts.[48] An explanation for this might be that the Ga(III)-TSC complex hydrolyzes within the cell and the free TSC ligand gets released, which in turn chelates intracellular iron and possibly also sequesters iron from the RNR enzyme.[45]

Herein we report on the synthesis, spectroscopic and X-ray diffraction studies, as well as evaluation of antiproliferative activity of two gallium(III) and one iron(III) complex resulting from reactions of gallium(III) and iron(II) salts/complexes with L-proline-thiosemicarbazone hybrids L-Pro-FTSC and dm-L-Pro-FTSC (Chart 1). In addition, solution equilibrium studies of the complexation of L-Pro-FTSC with gallium(III), iron(II) and iron(III) in aqueous solution have been performed by ^{1}H NMR spectroscopy, pH-potentiometry and UV–vis spectrophotometry. Speciation data were used to rationalize the cytotoxicity of the compounds tested in human cancer cell lines.

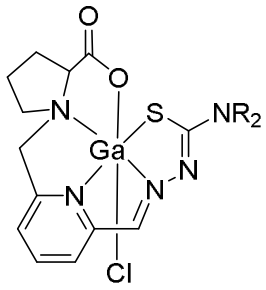

R = H, [GaCl(L-Pro-FTSC-2H)] (**1**)
R = CH_3, [GaCl(dm-L-Pro-FTSC-2H)] (**2**)

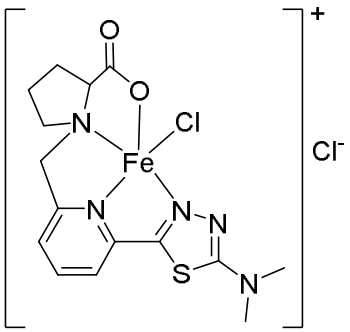

[FeCl(L-Pro-FTDA-H)]Cl (**3**)

Chart 1. Complexes studied in this work.

2. Experimental

2.1. Materials and Methods

L-Pro-FTSC,[49,50] dm-L-Pro-FTSC[51] and tetrapyridino-ferrous chloride[52] were prepared according to published protocols. Solvents were dried using standard techniques and/or degassed using the traditional freeze-pump-thaw method (three cycles) if needed.[53] KOH, $GaCl_3$, KSCN, EDTA, 4-(2-hydroxyethyl)-1-piperazineethanesulfonic acid (HEPES) and *N*-cyclohexyl-2-aminoethanesulfonic acid (CHES) were purchased from Sigma-Aldrich and HCl, KCl, $KMnO_4$, Fe, $FeCl_3$ were Reanal products. The iron(II) stock solution was obtained from fine Fe powder dissolved in a known amount of HCl solution under a purified, strictly oxygen-free argon atmosphere, then filtered, stored and used under anaerobic conditions. KSCN solution was used to check the absence of iron(III) traces in the iron(II) solution. The concentration of the iron(II) stock solution was determined by permanganometric titrations under acidic conditions. $GaCl_3$ and $FeCl_3$ stock solution were prepared by dissolving the appropriate amount of the metal

chlorides in a known amount of HCl and their concentrations were determined by complexometry via the EDTA complexes. Accurate strong acid content of the metal stock solutions were determined by pH-potentiometric titrations.

2.2. Synthesis of Complexes

2.2.1. [GaCl(L-Pro-FTSC–2H)]·0.7H_2O·0.5CH_3OH, **1**·0.7H_2O·0.5CH_3OH

To a solution of L-Pro-FTSC (0.10 g, 0.32 mmol) in dry methanol (5 mL) was added a solution of gallium chloride (281.7 mM in dry ethanol (EtOH)) (1.20 mL, 0.34 mmol) and triethylamine (0.15 mL, 1.05 mmol). The reaction mixture was stirred overnight at room temperature. The next day a yellow precipitate was filtered off, washed with dry methanol and dried in vacuo. Single-crystal X-ray diffraction quality crystals were obtained by slow diffusion of diethyl ether into a methanolic solution of **1** (c ≈ 5 mg mL^{-1}). Yield: 0.10 g, 73%. Anal. Calcd for $GaC_{13}H_{15}N_5ClO_2S$·0.7H_2O·0.5CH_3OH (M 439.16 g mol^{-1}): C, 36.92; H, 4.22; N, 15.95; S, 7.30. Found: C, 37.10; H, 3.84; N, 15.61; S, 7.22. ^{1}H NMR (500 MHz, DMSO-d_6) δ 8.43 (s, 1H, H^{13}), 8.20 (t, J = 7.8 Hz, 1H, H^5), 8.11 (s, 2H, H^3), 7.80 (d, J = 7.6 Hz, 1H, H^6), 7.56 (d, J = 7.8 Hz, 1H, H^4), 4.57 (d, J = 16.2 Hz, 1H, H^7), 4.43 (d, J = 16.6 Hz, 1H, H^7), 4.15 – 4.04 (m, 1H, H^{11}), 3.57 – 3.47 (m, 1H, H^8), 3.15 – 3.04 (m, 1H, H^{11}), 2.55 – 2.39 (m, 1H, H^9), 2.09 – 1.97 (m, 1H, H^{10}), 1.87 (m, 1H, H^9), 1.66 (m, 1H, H^{10}). ^{13}C NMR (126 MHz, DMSO-d_6) δ 179.99 (Cq, C^{14}), 173.25 (Cq, C^{12}), 149.76 (Cq, C^3), 143.90 (Cq, C^1), 143.39 (CH , C^5), 131.97 (CH, C^{13}), 123.17 (CH, C^6), 123.13 (CH, C^4), 69.47 (CH, C^8), 59.69 (CH_2, C^7), 57.99(CH_2, C^{11}), 31.89 (CH_2, C^9), 24.59 (CH_2, C_{10}). Solubility in water ≥18.28 mg mL^{-1}. ESI-MS (methanol), positive: m/z 374 ($[M - Cl]^+$). IR (ATR, selected bands, $\tilde{\nu}_{max}$): 3298, 3082, 1738, 1636, 1411, 1371, 1171, 1079, 1024, 653, 606 cm^{-1}.

2.2.2. [GaCl(dm-L-Pro-FTSC–2H)]·0.4H_2O, **2**·0.4H_2O

To a suspension of dm-L-Pro-FTSC (0.16 g, 0.48 mmol) in dry EtOH (10 mL) was added a solution of gallium chloride (281.7 mM in dry EtOH) (1.86 mL, 0.53 mmol) and triethylamine (0.22 mL, 1.59 mmol). A yellow, clear solution was formed, which was stirred overnight at 70 °C. The next day the solution was cooled to room temperature and subjected to slow diethyl ether diffusion, after which a yellow precipitate appeared which was filtered, washed with dry

ethanol and dried *in vacuo*. X-ray diffraction quality crystals were obtained after slow diffusion of diethyl ether into an EtOH/water (20:1) solution of **2** (c ≈ 5 mg mL^{-1}). Yield: 0.17 g, 79%. Anal. Calcd for $GaC_{15}H_{19}N_5O_2SCl \cdot 0.4H_2O$ (M 445.79 g mol^{-1}): C, 40.41; H, 4.48; N, 15.71; S, 7.19. Found: C, 40.45; H, 4.22; N, 15.34; S, 7.10. ^{1}H NMR (500 MHz, DMSO-d_6) δ 8.49 (s, 1H, H^{13}), 8.20 (t, J = 7.8 Hz, 1H, H^5), 7.78 (d, J = 7.8 Hz, 1H, H^6), 7.56 (d, J = 7.8 Hz, 1H, H^4), 4.57 (d, J = 16.4 Hz, 1H, H^7), 4.44 (d, J = 16.6 Hz, 1H, H^7), 4.17 – 4.06 (m, 1H, H^{11}), 3.53 (dd, J = 10.7, 4.9 Hz, 1H, H^8), 3.17 – 3.07 (m, 1H, H^{11}), 2.48 – 2.41 (m, 1H, H^9, overlapped with residual DMSO signal), 2.13 – 1.98 (m, 1H, H^{10}), 1.93 – 1.83 (m, 1H, H^9), 1.76 – 1.61 (m, 1H, H^{10}). ^{13}C NMR (126 MHz, DMSO-d_6) δ 178.75 (Cq, C^{14}), 173.23 (Cq, C^{12}), 149.78 (Cq, C^3), 144.03 (Cq, C^1), 143.45 (CH, C^5), 132.63 (CH, C^{13}), 123.13 (CH, C^4), 123.07 (CH, C^6), 69.40 (CH, C^8), 59.68 (CH_2, C_7), 58.01(CH_2, C^{11}), 40.96 – 38,89 ($2CH_3$, C^{16}, C^{15}, overlapped with residual DMSO signal) 31.94 (CH_2, C^9), 24.69 (CH_2, C^{10}). Solubility in water ≥11.67 mg mL^{-1}. ESI-MS (methanol), positive: m/z 402 ($[M - Cl]^+$). IR (ATR, selected bands, $\tilde{\nu}_{max}$): 2875, 1654, 1598, 1361, 1294, 1251, 1212, 1144, 905, 764, 676, 625 cm^{-1}.

2.2.2. [FeCl(L-Pro-FTDA–H)]Cl, **3**

To a solution of dm-L-Pro-FTSC (0.10 g, 0.30 mmol) in degassed methanol (5 mL) was added a solution of tetrapyridino-ferrous chloride (0.13 g, 0.30 mmol) in degassed methanol (5 mL). The color of the solution changed immediately from slightly yellow to dark blue and the reaction mixture was stirred overnight at room temperature. The reaction mixture was subjected to slow diethyl ether diffusion, using degassed diethyl ether. A blue-green precipitate was collected by filtration after several days. The mother liquor was allowed to stand for several days under an argon atmosphere. During this time its color changed from dark blue to purple and red-brown crystals appeared which were filtered and dried *in vacuo*. The obtained crystals were of X-ray diffraction quality. Yield: 25 mg, 16%. Anal. Calcd for $C_{15}H_{18}FeN_5O_2SCl_2 \cdot 1.5H_2O \cdot MeOH$ (M 518.22 g mol-1): C, 37.13; H, 4.87; N, 13.54; S, 6.18. Found: C, 36.85; H, 4.59; N, 13.19; S, 6.33.

2.3. Crystallographic Structure Determination

X-ray diffraction measurements were performed on a Bruker X8 APEXII CCD and Bruker D8-Venture diffractometers. Single crystal was positioned at 35, 40 and 35 mm from the detector, and 950, 1964 and 4113 frames were measured, each for 10, 30 and 10 s over 1° scan width for **1**, **2** and **3**, respectively. The data were processed using SAINT software.[54] Crystal data, data collection parameters, and structure refinement details are given in Table 1. The structure was solved by direct methods and refined by full-matrix least-squares techniques. Non-hydrogen atoms were refined with anisotropic displacement parameters. Hydrogen atoms were inserted in calculated positions and refined with a riding model. The following computer programs and hardware were used: structure solution, *SHELXS-97* and refinement, *SHELXL-97*;[55] molecular diagrams, ORTEP;[56] computer, Intel CoreDuo.

2.4. Cell lines and culture conditions

Human cervical carcinoma (HeLa), human alveolar basal adenocarcinoma (A549), human colorectal adenocarcinoma (LS174) cell lines and normal human fetal lung fibroblast cell line (MRC-5) were maintained as monolayer culture in the Roswell Park Memorial Institute (RPMI) 1640 nutrient medium (Sigma Chemicals Co, USA). RPMI 1640 nutrient medium was prepared in sterile deionized water, supplemented with penicillin (192 U/mL), streptomycin (200 mg/mL), HEPES (25 mM), L-glutamine (3 mM) and 10% of heat-inactivated foetal calf serum (FCS) (pH 7.2). The cells were grown at 37 ºC in 5% CO_2 in a humidified air atmosphere.

Table 1. Crystal Data and Details of Data Collection for **1**·0.175H_2O, **2**·H_2O and **3**

Compound	**1**·0.175H_2O	**2**·H_2O	**3**
empirical formula	$C_{13}H_{15.35}ClGaN_5O_{2.175}S$	$C_{15}H_{21}ClGaN_5O_3S$	$C_{15}H_{22}Cl_2FeN_5O_4S$
Fw	413.68	456.60	495.19
space group	*C*2	$P2_1$	$P2_12_12_1$
a, Å	30.5731(18)	8.2362(3)	7.4741(6)
b, Å	7.6058(4)	21.2237(8)	10.322(1)
c, Å	14.9814(8)	10.6393(4)	26.292(2)
β, °	113.394(2)	97.8388(12)	
V [Å^3]	3197.3(3)	1842.40(12)	2028.3(3)
Z	8	4	4
λ [Å]	0.71073	0.71073	0.71073
ρ_{calcd}, g cm^{-3}	1.719	1.646	1.622
cryst size, mm^3	0.18 × 0.02 × 0.02	0.16 × 0.12 × 0.05	0.15 × 0.15 × 0.01
T [K]	100(2)	100(2)	100(2)
μ, mm^{-1}	2.036	1.778	1.142
R_1[a]	0.0636	0.0252	0.0400
wR_2[b]	0.1082	0.0539	0.1037
GOF[c]	1.130	1.646	1.064
Flack parameter	0.022(18)	–0.004(4)	0.03(2)

[a] $R_1 = \Sigma||F_o| - |F_c||/\Sigma|F_o|$. [b] $wR_2 = \{\Sigma[w(F_o^2 - F_c^2)^2]/\Sigma[w(F_o^2)^2]\}^{1/2}$. [c] $GOF = \{\Sigma[w(F_o^2 - F_c^2)^2]/(n-p)\}^{1/2}$, where *n* is the number of reflections and *p* is the total number of parameters refined.

2.5. MTT assay

Antiproliferative activity of the investigated complexes was determined using 3-(4,5-dymethylthiazol-yl)-2,5-diphenyltetrazolium bromide (MTT, Sigma-Aldrich) assay.[57] Cells were seeded into 96-well cell culture plates (Thermo Scientific Nunc™), at a cell density of 4000 c/w (HeLa), 6000 c/w (A549), 7000 c/w (LS174), 5000 c/w (MRC-5) in 100 µL of culture medium. After 24 h of growth, cells were exposed to the serial dilutions of the tested complexes. The investigated compounds were dissolved in sterile water at a concentration of 10 mM as stock solution, and prior the use diluted with nutrient medium to the desired final concentrations (up to 300 µM). Samples at each concentration were tested in triplicates. After incubation periods of 48 h, 20 µL of MTT solution (5 mg/mL in phosphate buffer solution, pH 7.2) were added to each well. Samples were incubated for 4 h at 37 °C, with 5% CO_2 in a humidified atmosphere. Formazan crystals were dissolved in 100 µL of 10% sodium dodecyl sulfate (SDS). Absorbances were recorded after 24 h, on an enzyme-linked immunosorbent assay (ELISA) reader (ThermoLabsystems Multiskan EX 200–240 V), at the wavelength of 570 nm. The IC_{50} value, defined as the concentration of the compound causing 50% cell growth inhibition, was estimated from the dose-response curves.

2.6. pH-potentiometric measurements and calculations

The exact concentration of the stock solutions of the L-Pro-FTSC was determined from pH-potentiometric titrations by using the HYPERQUAD software.[58] The pH-potentiometric measurements for the determination of the proton dissociation constants of the L-Pro-FTSC and the overall stability constants of the iron(II) and iron(III) complexes were carried out at 298.0 ± 0.1 K in water and at an ionic strength of 0.10 M (KCl) to keep the activity coefficients constant. The titrations were performed with carbonate-free 0.10 M KOH solution. The concentrations of the base and the HCl were determined by pH-potentiometric titrations. An Orion 710A pH-meter equipped with a Metrohm combined electrode (type 6.0234.100) and a Metrohm 665 Dosimat burette were used for the titrations. The electrode system was calibrated to the pH = $-\log[H^+]$ scale according to the method suggested by Irving *et al.*[59] The average water ionisation constant pK_w is 13.76 ± 0.01, which corresponds well to the literature data.[60] The reproducibility of the titration points included in the calculations was within 0.005 pH. The pH-metric titrations were performed in the pH range 2.0 − 11.5. The initial volume of the samples was 5.0 mL. The ligand concentration was 2 mM and metal ion-to-ligand ratios of 1:1 − 1:4 were used. The accepted fitting of the titration curves was always

less than 0.01 mL. Samples were deoxygenated by bubbling purified argon through them for approximately 10 min prior to the measurements. Iron(II) was added to the samples in tightly closed vessels, which were prior completely deoxygenated by bubbling a stream of purified argon through them for *ca.* 20 min. Argon was also passed over the solutions during the titrations.

The protonation constants of the L-Pro-FTSC were determined with the computer program HYPERQUAD.[58] PSEQUAD[61] was utilised to establish the stoichiometry of the complexes and to calculate the stability constants ($\log\beta(M_pL_qH_r)$) using the literature data for iron(III) hydroxido complexes.[62] $\beta(M_pL_qH_r)$ is defined for the general equilibrium $p\mathrm{M} + q\mathrm{L} + r\mathrm{H} \rightleftharpoons M_pL_qH_r$ as $\beta(M_pL_qH_r) = [M_pL_qH_r]/[M]^p[L]^q[H]^r$, where M denotes the metal ion and L the completely deprotonated ligand. In all calculations exclusively titration data were used from experiments in which no precipitate was visible in the reaction mixture.

2.7. UV–vis spectrophotometric and ^{1}H NMR measurements

A Hewlett Packard 8452A diode array spectrophotometer was used to record the UV–vis spectra in the 200 to 800 nm window. The path length was 1.0 or 2.0 cm. The spectrophotometric titrations were performed on samples of the L-Pro-FTSC alone or with iron(II) and iron(III) ions; the concentration of the ligand was ~100 μM and the metal-to-ligand ratios were 1:1 and 1:2 over the pH range between 2 and 11.5 at an ionic strength of 0.10 M (KCl) in water at 298.0 ± 0.1 K. For iron(II) samples, spectra were recorded under anaerobic conditions. Time-dependence of UV–vis absorption spectra were recorded for the iron(III) – L-Pro-FTSC (1:1) system at pH 7.4 (10 mM HEPES) and 9.0 (10 mM CHES) under both aerobic and anaerobic conditions.

The pH-dependent ^{1}H NMR studies on the gallium(III) – L-Pro-FTSC (1:1) system were carried out on a Bruker Ultrashield 500 Plus instrument. 4,4-Dimethyl-4-silapentane-1-sulfonic acid was used as an internal NMR standard and WATERGATE method was used to suppress the solvent resonance. L-Pro-FTSC was dissolved in a 10% (v/v) D_2O/H_2O mixture in a concentration of 1 mM at 298 K and ionic strength of 0.10 M (KCl). PSEQUAD[61] was used to calculate the $\log\beta$ values of the complexes $[GaLH]^{2+}$ and $[GaL]^{+}$ using the literature data for gallium(III) hydroxido complexes.[63]

3. Results and Discussion

3.1. Synthesis and Characterisation of Metal Complexes

The synthesis of L-Pro-FTSC and dm-L-Pro-FTSC was reported recently.[49,51] The gallium(III) complexes [GaCl(L-Pro-FTSC–2H)]·0.7H_2O·0.5CH_3OH (**1**·0.7H_2O·0.5CH_3OH) and [GaCl(dm-L-Pro-FTSC–2H)]·0.4H_2O (**2**·0.4H_2O) were prepared by reaction of the corresponding ligand precursor with gallium(III) chloride in dry methanol and dry EtOH in the presence of trimethylamine as a base with yields of 73 and 79%, respectively. The structure and formulation of both complexes was confirmed by X-ray diffraction measurements (vide infra), one- and two-dimensional ^{1}H and ^{13}C NMR spectra and elemental analysis (see Experimental Section). ESI mass spectra of the gallium(III) complexes **1** and **2** showed peaks with *m*/*z* 374 and 402, respectively, attributed to the $[M - Cl]^+$ ion.

The synthesis of the corresponding iron(III) complexes turned out to be not as straightforward as was the case for gallium(III) complexes **1** and **2**. Reaction of iron(III) chloride with L-Pro-FTSC in methanol in air led to a red solution and degradation of the ligand. ESI mass spectra of the resulting product mixture were difficult to interpret. The same reaction under inert atmosphere led to a blue solution, implying the reduction of iron(III) to iron(II) with concomitant oxidation of the ligand. Iron(II) complexes with L-Pro-FTSC and dm-L-Pro-FTSC turned out to be extremely air sensitive and we were not able to obtain X-ray diffraction quality crystals for structure determination. The only isolated iron(III) complex was obtained by the reaction of trans-dichlorido(tetrapyridine)iron(II), also known as "yellow salt", with dm-L-Pro-FTSC in deoxygenated methanol. The initially obtained dark-blue solution was subjected to slow diffusion of diethyl ether which resulted in the precipitation of a blue-green solid (iron(II)complex). The mother liquor was left to stand for several days under argon atmosphere. During this time the color of the solution changed from blue to violet and red-brown crystals appeared. It seems that an oxidation took place in the presence of small amounts of oxygen which entered the Schlenk tube in which the mother liquor was stored. The ligand and the metal center were oxidised giving the six-coordinate iron(III)thiadiazole complex **3**, and its structure was confirmed by X-ray diffraction measurements and elemental analysis.

3.2. X-ray crystallography

The results of X-ray diffraction studies of complexes **1**–**3** are shown in Figures 1–3. The complexes **1** and **2** crystallised in the noncentrosymmetric monoclinic space groups *C*2 and $P2_1$, respectively, while **3** in the noncentrosymmetric orthorhombic space group $P2_12_12_1$. Unlike **3**, the asymmetric unit of **1** and **2** consists of two crystallographically independent molecules of complexes. The proline-thiosemicarbazone hybrids L-Pro-FTSC and dm-L-Pro-FTSC act as pentadentate doubly deprotonated ligands bonded to gallium(III) via pyridine nitrogen atom, imine nitrogen, thiolato sulfur atom, tertiary proline nitrogen, and proline carboxylate oxygen atom.

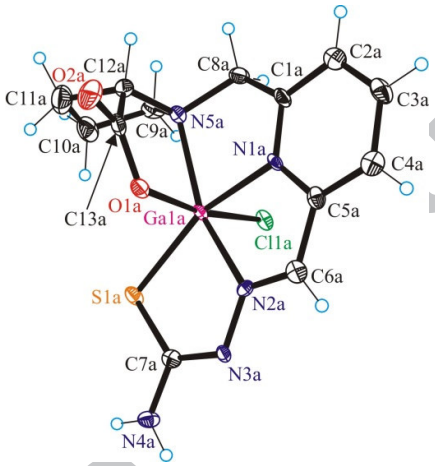

Figure 1. ORTEP view of **1** with thermal displacement ellipsoids drawn at 50% probability level. Selected bond distances (Å) and bond angles (deg): Ga1a–N1a 2.026(6), Ga1a–N2a 2.089(6), Ga1a–S1a 2.330(2), Ga1a–N5a 2.158(6) and Ga1a–O1a 1.977(5), Ga1a–Cl1a 2.349(2), N2a–N3a 1.356(8), C7a–S1a 1.750(8); N1a–Ga1a–N2a 77.2(2), N2a–Ga1a–S1a 82.68(18), N1a–Ga1a–N5a 79.8(2), N5a–Ga1a–O1a 81.5(2), N1a–Ga1a–O1a 86.9(2), N2a–Ga1a–O1a 89.3(2), S1a–Ga1a–O1a 92.57(16), O1a–Ga1a–Cl1a 170.47(17), N1a–Ga1a–Cl1a 89.60(17), N2a–Ga1a–Cl1a 98.59(17), N5a–Ga1a–Cl1a 89.20(17), S1a–Ga1a–Cl1a 93.77(7).

This mode of coordination of $(\text{L-Pro-FTSC}-2\text{H})^{2-}$ $(\text{dm-L-Pro-FTSC}-2\text{H})^{2-}$ is well-documented for copper(II) and zinc(II).[49]

The coordination geometry of gallium(III) in **1** and **2** can be described as distorted octahedral with atoms N1a, N2a, S1a and N5a forming the equatorial plane and O1a and the chloride ligand Cl1a in axial positions (Figures 1 and 2). Upon coordination of the pentadentate ligand to gallium(III) four five-membered chelate rings are formed, three of which are essentially planar, while the fourth prolinic moiety adopts a half-chair conformation. The metal–TSC

bonds Ga1a–N1a and Ga1a–S1a (see legend to Figure 2) are significantly (> 3σ) shorter, while Ga1a–N2a bond is significantly longer than analogous interatomic distances in $[GaL_2][GaCl_4]$ (HL = 2-acetylpyridine ^{4}N-dimethylthiosemicarbazone).[64]

As also in copper(II) and zinc(II) complexes with L-Pro-FTSC derivatives, the L-prolinate nitrogen atom N5a, in addition to C12a (or C14a), becomes a chiral center. The prolinate nitrogen atom and the asymmetric carbon atom adopt opposite configurations (S_C,R_N). Similar examples that resulted from coordination to metal ion or protonation of the proline nitrogen were reported, but they are rare.[65]

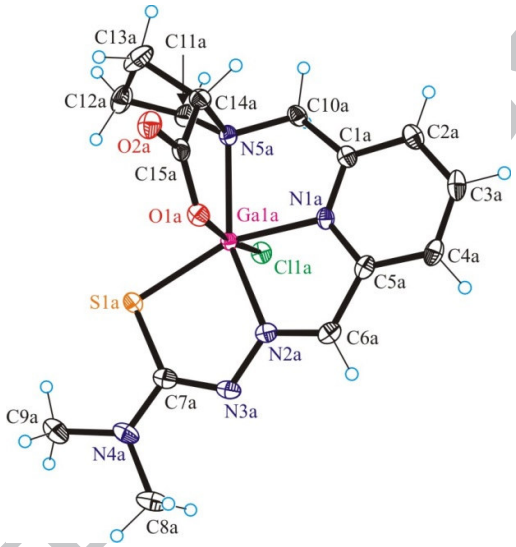

Figure 2. ORTEP view of **2** with thermal displacement ellipsoids drawn at 50% probability level. Selected bond distances (Å) and bond angles (deg): Ga1a–N1a 1.9932(12), Ga1a–N2a 2.0756(15), Ga1a–S1a 2.3304(4), Ga1a–N5a 2.1525(15) and Ga1a–O1a 1.9932(12), Ga1a–Cl1a 2.3909(4), N2a–N3a 1.345(2), C7a–S1a 1.755(2); N1a–Ga1a–N2a 77.06(6), N2a–Ga1a–S1a 82.94(5), N1a–Ga1a–N5a 79.37(6), N5a–Ga1a–O1a 81.88(6), N1a–Ga1a–O1a 89.94(6), N2a–Ga1a–O1a 89.65(6), S1a–Ga1a–O1a 90.46(4), O1a–Ga1a–Cl1a 171.51(4), N1a–Ga1a–Cl1a 88.75(4), N2a–Ga1a–Cl1a 98.22(4), N5a–Ga1a–Cl1a 89.64(4), S1a–Ga1a–Cl1a 93.640(16).

A feature of note in the crystal structure of **1** is the formation of pairs of crystallographically independent molecules of complexes via strong hydrogen bonds of the type N–H···N (see Figure S1). Other hydrogen bonds and their parameters are listed in Table S1. Complex **2** is not able to form this kind of pairs since by terminal dimethylation of the thiosemicarbazone moiety, the ligand loses its ability to act as proton donor through intermolecular hydrogen

bonding interactions. Hydrogen bonds which are still present in the crystal structure of **2** are given in Table S2.

The new compound formed in the presence of iron(II/III) ions acts as a monodeprotonated pentadentate ligand providing three donor atoms for the equatorial plane completed by a chlorido ligand and a carboxylate ligand in an axial position. The latter plays a role of a bridging ligand with formation of a monocationic chain of six-coordinate iron(III) complex **3** the global charge of which is counterbalanced by chloride ions.

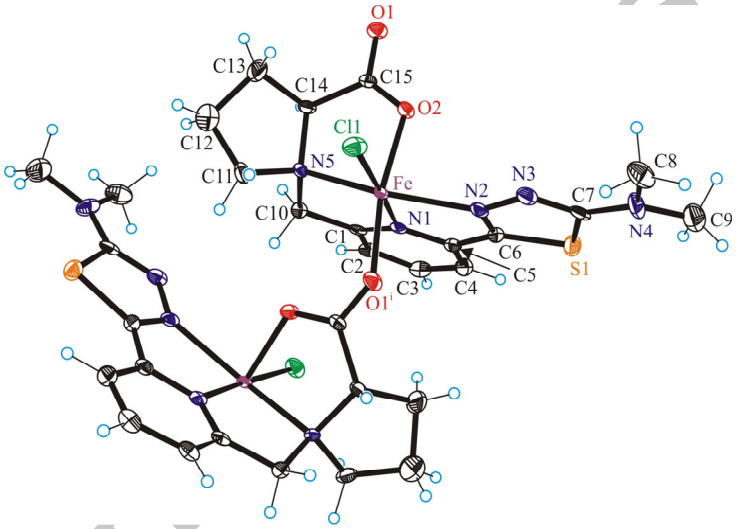

Figure 3. ORTEP view of a fragment of the crystal structure of **3** with thermal displacement ellipsoids drawn at 50% probability level showing the formation of a cationic polymeric chain. Selected bond distances (Å) and bond angles (deg): Fe–N1 2.134(3), Fe–N2 2.192(3), Fe–O2 2.072(3), Fe–N5 2.257(3) and Fe–O1^{i} 2.053(3) (i denotes atom generated by symmetry transformation $-x + 1$, $y + 0.5$, $-z + 0.5$) and Fe–Cl1 2.3089(12), N2–N3 1.370(5), C6–S1 1.736(4), C7–S1 1.769(4); N1–Fe–N2 74.78(13), N1–Fe–N5 75.21(12), N5–Fe–O2 79.11(11), N1–Fe–O2 86.79(11), N2–Fe–O2 83.41(12), Cl1–Fe–O2 91.87(9), O2–Fe–O1^{i} 169.06(12), Cl1–Fe–N2 108.31(10), Cl1–Fe–N5 101.35(9), N2–Fe–O1^{i} 85.84(12), N1–Fe–O1^{i} 88.43(12), N5–Fe–O1^{i} 109.13(11).

Oxidative addition of sulfur atom to the carbon atom of the neighbouring C=N bond led to formation of a five-membered thiadiazole ring. The formation of 1,3,4-thiadiazole ring via oxidative cyclisation of the thiosemicarbazones, dithiocarbazate or thiocarbohydrazones has been mainly observed in the presence of iron(III) and copper(II),[66] although cyclisations

induced by silver(I), zinc(II), cadmium(II)[67] and vanadium(IV/V)[68] were also reported. Although the mechanism of ring formation has not been resolved yet, it certainly implies the coordination of the metal cation as a Lewis acid at the imine nitrogen atom, followed by the nucleophilic attack of thiol sulfur on the imine carbon and ring closure, and finally by the electron abstracting-dehydrogenation step.[68c]

The lack of proton donor groups in the coordinated ligand reduces strongly the possibilities for hydrogen bonding in the crystal structure of **3**. Only the two co-crystallised water molecules are involved in hydrogen bonding between themselves or by acting as proton donors in H-bond formation with chlorido ligand and chloride counterion (Table S3).

3.3. Cytotoxicity of complexes

Complexes **1–3** were examined using the MTT assay in order to evaluate their antiproliferative activity *in vitro*. The analysis was performed in several human neoplastic cell lines (HeLa, A549, LS174), and one human fetal lung fibroblast cell line (MRC-5), which was used as a noncancerous model for the *in vitro* toxicity evaluation. The results are summarized in Table 2 in terms of IC_{50} values for the 48 h incubation period, which are calculated as mean values obtained from two to three independent experiments and quoted with their standard deviations.

Cytotoxicity data indicate poor antiproliferative activity of **1** and **3** (IC_{50} > 300 μM), while **2** showed higher cytotoxicity, with IC_{50} values being in the range of 50–100 μM. The most sensitive cell line was shown to be the colorectal adenocarcinoma cell line LS174 (IC_{50}(**2**)= 54.5 ± 2.6 μM). Comparison of the data for ligand precursors, L-Pro-FTSC and dm-L-Pro-FTSC, with those of **1** and **2** suggested that complexation with L-proline-thiosemicarbazone hybrids to gallium(III) showed better activity *in vitro* than complexation to iron. An explanation for this might be that the gallium(III)-TSC complex hydrolyses within the cell and the free TSC ligand gets released, which in turn chelates intracellular iron and possibly also sequesters iron from the RNR enzyme.[48] Also, comparing the IC_{50} values of **1** and **2** has shown that dimethylation enhanced antiproliferative activity, which is in accordance with the previously reported studies which revealed how dimethylation of terminal aminogroup affects the cytotoxicity of ligands alone and/or complexes.[49,69]

Table 2. IC_{50} [μM] (mean ± SD) for **1**–**3** and ligand precursors[51] in human cancer and noncancerous cell lines after 48 h incubation time.

Compound	HeLa	A549	LS174	MRC5
1	>300	>300	>300	>300
2	122.0 ± 4.8	103.1 ± 2.0	54.5 ± 2.6	87.0 ± 3.5
3	>300	268.5 ± 5.3	54.5 ± 2.6	87.0 ± 3.5
L-Pro-FTSC	>300	>300	n.d.	>300
dm-L-Pro-FTSC	224.6 ± 6.4	204.3 ± 4.8	n.d.	178.4 ± 1.5

3.4. Solution stability of the complexes

Solution equilibrium studies on the complexation of L-Pro-FTSC as a reference compound with gallium(III), iron(II) and iron(III) ions were performed. Aqueous solution stability of the complexes formed in water was characterised and compared. The knowledge of speciation, especially at physiological pH, is a mandatory prerequisite for understanding the most plausible chemical forms of the complexes in solution which may be responsible for the biological activity. On the other hand, the binding ability of TSCs to iron(II) deserves a particular attention, since formation of an intracellular iron complex plays a crucial role in the suggested mechanism of inhibition of the RNR enzyme.[70]

The proton dissociation processes of L-Pro-FTSC were already investigated in our recent work[50] and the pK_a values obtained here were found to be identical with the previously reported (Table 3). It is worth noting that L-Pro-FTSC is practically neutral at pH 7.4 (96% H_2L and 4% HL^-, where L^{2-} is the fully deprotonated form of the ligand precursor). However, H_2L adopts a zwitterionic structure with COO^- and $N_{Pro}H^+$, which explains its excellent aqueous-solubility. ^{1}H NMR spectroscopy was found to be an adequate method to follow the complex formation processes of L-Pro-FTSC with gallium(III) ions. The ^{1}H NMR spectra recorded at various pH values and 1:1 metal-to-ligand ratio (Figure 4a) reveal slow ligand-exchange processes with respect to the NMR time scale as the chemical shifts of the protons of the ligand precursor and ligand coordinated to gallium(III) were observed separately. The integrated peak areas of the C*H*=N protons were converted to molar fractions of the ligand (Figure 4b). It can be seen from Figure 4b that complexes are formed only between pH 2 and pH 7 since no metal-bound ligand could be detected outside this range. Parallel to the decomposition of the gallium(III) complex with increasing pH, the upfield shift of the peaks

of the bound portion of the ligand is also observed indicating the deprotonation of the complex, thus the pK_a was determined on the basis of this pH-dependent shift (Table 3). Comparing the pK_a value of the complex with pK_2 and pK_3 of the ligand (pK_a << pK_2), the coordination of both the thiosemicarbazide and the Pro moieties is suggested in accordance with the result of the X-ray diffraction analysis of **1** (Figure 1). Thus formation of species $[GaLH]^{2+}$ and $[GaL]^{+}$ is assumed and their overall stability constants were calculated based on the ^{1}H NMR data (Table 3). At excess ligand precursor, only species already identified in the measurements at 1:1 metal-to-ligand ratio were found. Therefore formation of bis-ligand complexes was excluded. The binding ability of L-Pro-FTSC to gallium(III) was compared to that of 2-formylpyridine thiosemicarbazone (FTSC), the simplest α(N)-pyridyl TSC, and its N-terminally dimethylated derivative (pyridine-2-carboxaldehyde N^4,N^4-dimethylthiosemicarbazone, PTSC) via the calculated molar fractions of the ligands under identical conditions (Figure 4b). The L-Pro-FTSC forms higher stability complexes with gallium(III) ions than FTSC, though the complexes of both ligands decompose completely at the physiological pH. The decomposition is assumed to be even more pronounced upon dilution. This is presumably the reason for the similar IC_{50} values of these ligand precursors and their metal complexes (in the case of L-Pro-FTSC both are inactive against the tested human cancer cell lines, Table 2). On the other hand the N-terminal dimethylation significantly increases the solution stability of the gallium(III) complexes (*c.f.* molar fractions calculated for FTSC and PTSC), and higher stability is also expected for the complexes of dm-L-Pro-FTSC compared to that of L-Pro-FTSC. Most probably, the increased stability leads to the higher cytotoxicity of the gallium(III) complex (**2**) in comparison to that of the ligand precursor (Table 2). Thus the biological activity of the dm-L-Pro-FTSC complex is not governed simply by the ligand.

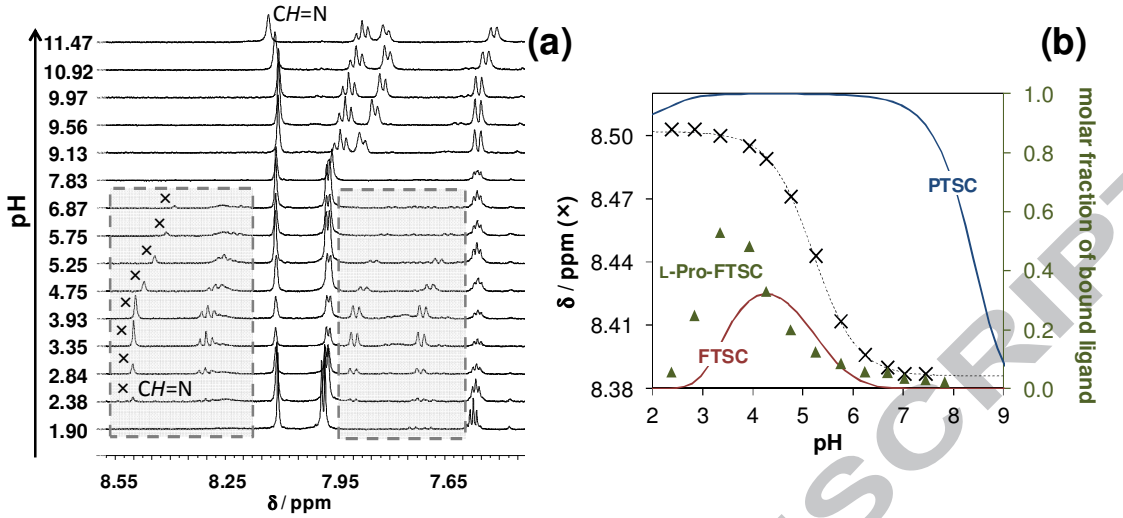

Figure 4. (a) Low field region of the ^{1}H NMR spectra of the gallium(III) – L-Pro-FTSC (1:1) system recorded at indicated pH values, and the framed details of spectra with dashed line indicate the peaks assigned to the protons of the bound ligand; (b) pH-dependence of the ^{1}H NMR chemical shifts of the C*H*=N peaks (×) with the fitted curve (dashed line) and the molar fractions of the bound ligand (▲) calculated on the basis of the integrals of these protons. Molar fractions calculated for metal-bound ligands FTSC and PTSC (solid lines) are shown for comparison based on the stability data taken from Ref. 69. [c_L = 1.0 mM; Ga:L = 1:1; T = 298 K and I = 0.10 M (KCl); 10% (v/v) D_2O]

Table 3. Cumulative ($\log\beta$ ($M_pL_qH_r$)) and derived stability constants of the iron(II)–, iron(III)–, and gallium(III)– L-Pro-FTSC complexes[a] [T = 298 K and I = 0.10 M (KCl)]

	gallium(III)[b]	iron(II)[c]	iron(III)[c]
$\log\beta$ [MLH]	20.9(1)	17.84(6)	21.16(3)
$\log\beta$ [ML]	15.7(1)	11.97(5)	17.73(4)
$\log\beta$ [MLH_{-1}]	–	1.25(9)	–
pK_a [MLH]	5.2	5.87	3.43
pM[d]	6.0	7.9	–

[a] Charges of the complexes are omitted for clarity. The numbers in parentheses are standard deviations. Proton dissociation constants of the ligand: pK_1 = 1.86, pK_2 = 8.78 and pK_3 = 11.08 taken from Ref. 50. [b] $\log\beta$ values calculated from the ^{1}H NMR δ values of the C*H*=N protons of the bound ligand. [c] $\log\beta$ values determined by pH-potentiometry. [d] pM = –log [unbound metal ions] at pH 7.40; c_L/c_M = 10; c_M = 0.001 mM. pM = 10.71 for iron(II) – FTSC; 11.6 for iron(II) – Triapine; 12.9 for iron(II) – PTSC systems based on data published in Ref. 69.

Complex formation of L-Pro-FTSC with iron(II) and iron(III) in aqueous solution was investigated by pH-potentiometry and UV–vis spectrophotometry. Stoichiometries and cumulative stability constants of the metal complexes furnishing the best fits to the experimental pH-potentiometric data are listed in Table 3. Formation of only mono-ligand

species was detected in the case of the iron(II/III) ions similarly to gallium(III), copper(II),[49] zinc(II)[48] and nickel(II).[48] Representative titration curves (Figure 5) reveal that complex formation processes start at higher pH in the case of iron(II), consequently iron(II) complexes possess lower stability constants than the corresponding iron(III) species. It should be noted that the ligand was not able to keep iron(II) in solution at a metal-to-ligand ratio of 1:1 at pH > 10, and precipitation occurred. Most probably concomitant with the hydrolysis of the complex (*i.e.* formation of $[FeLH_{-1}]$), significant complex decomposition also takes place in the basic pH range and the hydrolysis of the non-bound metal ion resulted in precipitation of iron hydroxide. The iron(II) complex formation is witnessed by absorbance changes in the wavelength range 220 − 430 nm at pH > 4 (Figure S1). Note that the formation of the green bis-ligand iron(II) complexes of TSCs is accompanied by the development of a typical broad absorption band with a maximum at ~520 nm,[69] which was not seen for the iron(II) - L-Pro-FTSC system. Most probably only mono-ligand iron(II) complexes are present in solution, in which the ligand acts as a pentadentate one, as also observed for the other metal ions studied. Binding through N_{pyr}, N, S^-, COO^- and N_{Pro} donor atoms is assumed in the complex [Fe(II)L], while in $[Fe(II)LH]^+$ the non-coordinating hydrazinic N is most probably protonated, and $[Fe(II)LH_{-1}]^-$ is a mixed hydroxido complex (= $[Fe(II)L(OH)]^-$). It should also be pointed out that α(N)-pyridyl TSCs generally form relatively stable octahedral bis-ligand complexes with iron(II), in which the ligands coordinate via the N_{pyr},N,S^- donor set.[69,71] However, the presence of the Pro moiety in the ligand L-Pro-FTSC seems to hinder the simultaneous binding of two ligands to the metal ion. The binding ability of TSCs to iron(II) can be easily compared at pH 7.4 by the calculation of pM values (Table 3). The lower pM value obtained for L-Pro-FTSC than those for FTSC, Triapine or PTSC indicates a weaker chelating ability of the former, which might be responsible for the inactivity of the ligand L-Pro-FTSC against the cancer cells.

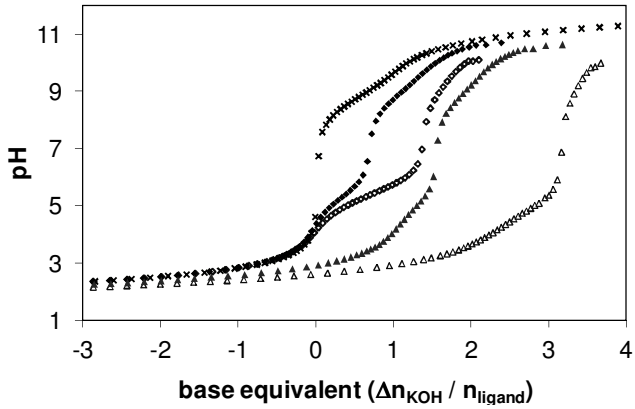

Figure 5. Representative pH-potentiometric titration curves for ligand L-Pro-FTSC (×), iron(II)–ligand system at 1:1 (◊) and 1:2 (♦), iron(III)– ligand system at 1:1 (Δ) and 1:2 (▲) metal-to-ligand ratios [c_L = 1.80 mM; T = 298 K and I = 0.10 M (KCl) in water]. *Negative base equivalent values mean an excess amount of acid.*

The stability of the iron(II) complexes of L-Pro-FTSC was also compared to that for other divalent first-row transition metal ions which form complexes with similar coordination geometry (Figure 6) and it follows the well-known Irving–Williams sequence.

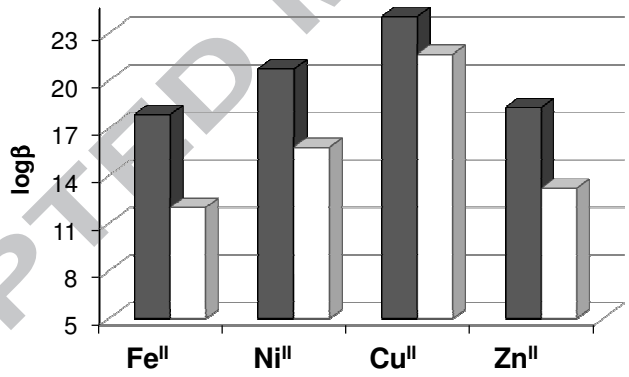

Figure 6. Cumulative stability constants (logβ) of the $[MLH]^+$ (grey bars) and [ML] (white bars) complexes of bivalent metal ions formed with L-Pro-FTSC [T = 298 K and I = 0.10 M (KCl)]. *Data for nickel(II), zinc(II) and copper(II) complexes are taken from Refs.49,51.*

The interaction of iron(III) with L-Pro-FTSC in aqueous solution was found to be rather complex, since a redox reaction was observed at pH ~7. Therefore, the stability constants (Table 3) were calculated from the data collected only at acidic pH values. Time-dependence of UV–vis spectra recorded at pH 7.4 (Figure 7a) revealed a slow change of the absorbance values and no differences were observed in the presence or absence of oxygen (Figure 7b). In order to monitor the presence of iron(II) in solution a qualitative colour reaction was used,

namely 2,2-bipyridine (bpy) was added to the solution containing iron(III) and L-Pro-FTSC at pH 7.4 (Figure S2). Bpy is known to form stable complexes with iron(II) with characteristic red colour. Sample containing iron(II) and L-Pro-FTSC was also tested. The red coloured iron(II)-bpy complex was formed undoubtedly in the iron(III) – L-Pro-FTSC system showing the presence of iron in oxidation sate +2, which is available for complexation with bpy. In the case of the iron(II) – L-Pro-FTSC system the red colour is much less intense, bpy can not compete so efficiently with L-Pro-FTSC for the binding to iron(II). Most probably L-Pro-FTSC is oxidised by iron(III) already at pH 7.4 according to the redox reaction shown in Scheme S1. Formation of the five-membered thiadiazole ring is probable and this oxidised product seems to be a weaker iron(II) binder than the original ligand precursor L-Pro-FTSC. Similar changes in UV–vis spectra were observed at pH 9, however, parallel to the slow redox reaction, decomposition of the complex also takes place resulting in the liberation of the ligand precursor and precipitation of iron(III)-hydroxides.

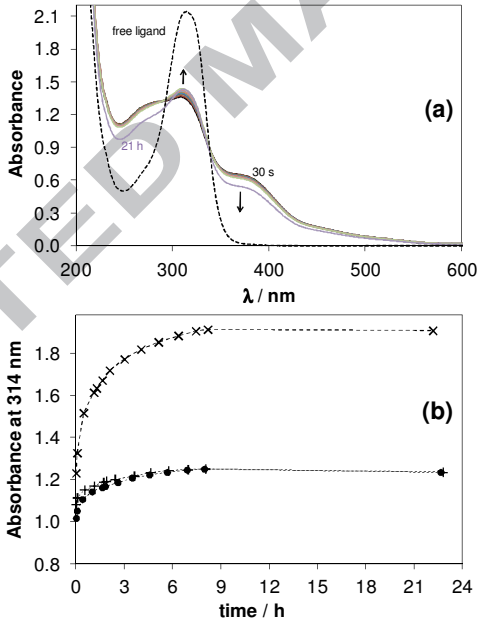

Figure 7. (a) Time-dependence of UV–vis absorbance spectra of iron(III) – L-Pro-FTSC (1:1) system (solid lines) and spectrum of the ligand (dashed line) recorded at pH 7.4. (b) Absorbance values measured at 314 nm for the iron(III) – L-Pro-FTSC system under anaerobic conditions at pH 7.4 (+) and 9.0 (×) and under aerobic conditions at pH 7.4 (●) plotted against the reaction time (b). [c_L = 100 μM; Fe:L = 1:1; pH 7.4 (10 mM HEPES), pH 9.0 (10 mM CHES); T = 298 K and I = 0.10 M (KCl); l = 2 cm]

4. Concluding remarks

Two gallium(III) complexes with pentadentate ligands, namely L-proline-thiosemicarbazone hybrids L-Pro-FTSC and its N-terminally dimethylated derivative, dm-L-Pro-FTSC, along with one iron(III) complex with a ligand derived from oxidation of L-Pro-FTSC, have been synthesised and spectroscopically characterised. In addition, their crystal structures were established by single crystal X-ray crystallography. The solution speciation of gallium(III), iron(II) and iron(III) complexes of L-Pro-FTSC has been characterized in pure aqueous solution via a combined approach using ^{1}H NMR spectroscopy, pH-potentiometry and UV−vis spectrophotometry. The hybrid compounds were found to act as a pentadentate ligand in solution coordinating to gallium(III) via the N_{pyr}, N, S^{-}, COO^{-} and N_{Pro} donor atoms. This binding mode was confirmed by X-ray crystallography in complexes **1** and **2**. Compounds prepared in this work were tested for antiproliferative activity in different human cancer cell lines. The low iron(II) binding affinity of L-Pro-FTSC most probably contributes to the low antiproliferative effect of the ligand precursor. The gallium(III) speciation data revealing low aqueous solution stability of the complex of L-Pro-FTSC, explain the lack of antiproliferative activity for complex **1**. Redox reaction between iron(III) and the ligands was detected at neutral and basic pH values resulting in the oxidation of the ligands possessing a five-membered thiadiazole ring.

Acknowledgements

Financial support of the FWF (Austrian Science Fund), project number P28223 is kindly acknowledged. This work was also supported by the Hungarian Research Foundation OTKA project PD103905 and the János Bolyai Research Scholarship of the Hungarian Academy of Sciences.

Supplementary material

CCDC-1452613, -1452614 and -1452615 contain the supplementary crystallographic data for this paper. These data can be obtained free of charge on application to The Director, CCDC, 12 Union Road, Cambridge CB2 1EZ, UK (email: deposit@ccdc.cam.ac.uk).

References

[1] C. R. Chitambar, *Expert Opin Investig Drugs* 13 (2004) 531–541.

[2] C. R. Chitambar, *Curr. Opin. Oncol.* 16 (2004) 547–552.

[3] B. J. Foster, K. Clagett-Carr, D. Hoth, B. Leyland-Jones, *Cancer Treat. Rep.* 70 (1986) 1311–1319.

[4] A. Y. Bedikian, M. Valdivieso, G. P. Bodey, M. A. Burgess, R. S. Benjamin, S. Hall, E. J. Freireich, *Cancer Treat. Rep.* 62 (1978) 1449–1453.

[5] M. K. Samson, R. J. Fraile, L. H. Baker, R. O'Bryan, *Cancer Clin. Trials* 3 (1980) 131–136.

[6] R. P. Jr. Warrell, R. S. Bockman, C. J. Coonley, M. Isaacs, H. Staszewski, *J. Clin. Invest.* 73 (1984) 1487–1490.

[7] L. R. Bernstein, *Pharmacol. Rev.* 50 (1998) 665–682.

[8] H. O. Habashy, D. G. Powe, C. M. Staka, E. A. Rakha, G. Ball, A. R. Green, M. Aleskandarany, E. C. Paish, R. Douglas Macmillan, R. I. Nicholson, I. O. Ellis, J. M. W. Gee, *Breast Cancer Res. Treat.* 119 (2010) 283–293.

[9] S. Kvaloey, R. Langholm, O. Kaalhus, T. Michaelsen, S. Funderud, A. F. Abrahamsen, T. Godal, *Int. J. Cancer* 33 (1984) 173–177.

[10] N. W. Smith, G. M. Strutton, M. D. Walsh, G. R. Wright, G. J. Seymour, M. F. Lavin, R. A. Gardiner, *Br. J. Urol.* 65 (1990) 339–344.

[11] J. Clausen, C. J. Edeling, J. Fogh, *Cancer Res.* 34 (1974) 1931–1937.

[12] P. Hoffer, *J. Nucl. Med.* 21 (1980) 394–398.

[13] S. V. Torti, F. M. Torti, *Cancer Res.* 71 (2011) 1511–1514.

[14] M. Kolberg, K. R. Strand, P. Graff, K. Kristoffer Andersson, *Biochim. Biophys. Acta, Proteins Proteomics* 1699 (2004) 1–34.

[15] J. Narasimhan, W. E. Antholine, C. R. Chitambar, *Biochem. Pharmacol.* 44 (1992) 2403–2408.

[16] P. Collery, H. Millart, D. Lamiable, R. Vistelle, P. Rinjard, P. G. Tran, B. Gourdier, C. Cossart, J. C. Bouana, C. Pechery, *Anticancer Res.* 9 (1989) 353–356.

[17] C. R. Chitambar, W. E. Antholine, *Antioxid. Redox Signaling* 18 (2013) 956–972.

[18] (a) J. A. Lessa, M. A. Soares, R. G. dos Santos, I. C. Mendes, L. B. Salum, H. N. Daghestani, A. D. Andricopulo, B. W. Day, A. Vogt, H. Beraldo, *BioMetals* 26 (2013)

151–165; (b) N. Zhang, Y. Tai, M. Li, P. Ma, J. Zhao, J. Niu, *Dalton Trans.* 43 (2014) 5182–5189.

[19] (a) F. Bacher, V. B. Arion, in: J. Reedijk (Ed.), Ruthenium Compounds as Antitumor Agents: New Developments, *Elsevier Reference Module in Chemistry, Molecular Sciences and Chemical Engineering*, Elsevier, Waltham, MA, 2014, http://dx.doi.org/10.1016/B978-0-12-409547-2.11353-8; (b) H. Beraldo, D. Gambino, *Mini-Rev. Med. Chem.* 4 (2004) 31–39.

[20] D. C. Reis, A. A. R. Despaigne, J. G. Da Silva, N. F. Silva, C. F. Vilela, I. C. Mendes, J. A. Takahashi, H. Beraldo, *Molecules* 18 (2013) 12645–12662.

[21] D. C. Quenelle, K. A. Keith, E. R. Kern, *Antiviral Res.* 71 (2006) 24–30.

[22] M. A. Salam, M. A. Affan, M. A. Arafat, R. Saha, R. Nasrin, *Heteroat. Chem.* 24 (2013) 43–52.

[23] A. Molter, J. Rust, C. W. Lehmann, G. Deepa, P. Chiba, F. Mohr, *Dalton Trans.* 40 (2011) 9810–9820.

[24] S. Arora, S. Agarwal, S. Singhal, *Int. J. Pharm. Pharm. Sci.* 6 (2014) 34–41.

[25] E. Ravina, *The evolution of drug discovery: from traditional medicines to modern drugs*, Weinheim: Wiley-VCH, 2011.

[26] R. W. Brockman, J. R. Thomson, M. J. Bell, H. E. Skipper, *Cancer Res.* 16 (1956) 167–170.

[27] S. Wadler, D. Makower, C. Clairmont, P. Lambert, K. Fehn, M. Sznol, *J. Clin. Oncol.* 22 (2004) 1553–1563.

[28] J. Kolesar, R. C. Brundage, M. Pomplun, D. Alberti, K. Holen, A. Traynor, P. Ivy, G. Wilding, *Cancer Chemother. Pharmacol.* 67 (2011) 393–400.

[29] C. M. Nutting, C. M. L. van Herpen, A. B. Miah, S. A. Bhide, J. P. Machiels, J. Buter, C. Kelly, D. de Raucourt, K. J. Harrington, *Ann. Oncol.* 20 (2009) 1275–1279.

[30] M. J. Mackenzie, D. Saltman, H. Hirte, J. Low, C. Johnson, G. Pond, M. J. Moore, *Invest. New Drugs* 25 (2007) 553–558.

[31] S. Attia, J. Kolesar, M. R. Mahoney, H. C. Pitot, D. Laheru, J. Heun, W. Huang, J. Eickhoff, C. Erlichman, K. D. Holen, *Invest. New Drugs* 26 (2008) 369–379.

[32] A. M. Traynor, J.-W. Lee, G. K. Bayer, J. M. Tate, S. P. Thomas, M. Mazurczak, D. L. Graham, J. M. Kolesar, J. H. Schiller, *Invest. New Drugs* 28 (2010) 91–97.

[33] J. J. Knox, S. J. Hotte, C. Kollmannsberger, E. Winquist, B. Fisher, E. Eisenhauer, *Invest. New Drugs* 25 (2007) 471–477.

[34] F. J. Giles, P. M. Fracasso, H. M. Kantarjian, J. E. Cortes, R. A. Brown, S. Verstovsek, Y. Alvarado, D. A. Thomas, S. Faderl, G. Garcia-Manero, L. P. Wright, T. Samson, A. Cahill, P. Lambert, W. Plunkett, M. Sznol, J. F. DiPersio, V. Gandhi, *Leuk. Res.* 27 (2003) 1077–1083.

[35] J. E. Karp, F. J. Giles, I. Gojo, L. Morris, J. Greer, B. Johnson, M. Thein, M. Sznol, J. Low, *Leuk. Res.* 32 (2008) 71–77.

[36] J. F. Zeidner, J. E. Karp, A. L. Blackford, B. D. Smith, I. Gojo, S. D. Gore, M. J. Levis, H. E. Carraway, J. M. Greer, S. P. Ivy, K. W. Pratz, M. A. McDevitt, *Haematologica* 99 (2014) 672–678.

[37] A. C. Sartorelli, E. C. Moore, M. S. Zedeck, K. C. Agrawal, *Biochemistry* 9 (1970) 4492–4498.

[38] F. A. French, E. J. Jr, Blanz, S. C. Shaddix, R. W. Brockman, *J. Med. Chem.* 17 (1974) 172–181.

[39] J. L. Nitiss, *Nat. Rev. Cancer* 9 (2009) 327–337.

[40] A. J. Schoeffler, J. M. Berger, *Q. Rev. Biophys.* 41 (2008) 41–101.

[41] J. Easmon, G. Puerstinger, G. Heinisch, T. Roth, H. H. Fiebig, W. Holzer, W. Jaeger, M. Jenny, J. Hofmann, *J. Med. Chem.* 44 (2001) 2164–2171.

[42] L. Wei, J. Easmon, R. K. Nagi, B. D. Muegge, L. A. Meyer, J. S. Lewis, *J. Nucl. Med.* 47 (2006) 2034–2041.

[43] A. M. Merlot, D. S. Kalinowski, D. R. Richardson, *Antioxid. Redox Signal* 18 (2013) 973–1006.

[44] L. Zhu, B. Zhou, X. Chen, H. Jiang, J. Shao, Y. Yun, *Biochem. Pharmacol.* 78 (2009) 1178–1185.

[45] A. Popovic-Bijelic, C. R. Kowol, M. E. S. Lind, J. Luo, F. Himo, E. A. Enyedy, V. B. Arion, A. Gräslund, *J. Inorg. Biochem.* 105 (2011) 1422–1431.

[46] Y. Aye, M. J. C. Long, J. Stubbe, *J. Biol. Chem.* 287 (2012) 35768–35778.

[47] B. M. Zeglis, V. Divilov, J. S. Lewis, *J. Med. Chem.* 54 (2011) 2391–2398.

[48] C. R. Kowol, R. Berger, R. Eichinger, A. Roller, M. A. Jakupec, P. P. Schmidt, V. B. Arion, B. K. Keppler, *J. Med. Chem.* 50 (2007) 1254–1265.

[49] F. Bacher, O. Dömötör, M. Kaltenbrunner, M. Mojovic, A. Popovic-Bijelic, A. Gräslund, A. Ozarowski, L. Filipović, S. Radulović, É. A. Enyedy, V. B. Arion, *Inorg. Chem.* 53 (2014) 12595–12609.

[50] G. Paolucci, A. Zanella, M. Bortoluzzi, S. Sostero, P. Longo, M. Napoli, *J. Mol. Catal. A: Chem.* 272 (2007) 258–264.

[51] F. Bacher, E. A. Enyedy, N. V. Nagy, A. Rockenbauer, G. M. Bognar, R. Trondl, M. S. Novak, E. Klapproth, T. Kiss, V. B. Arion, *Inorg. Chem.* 52 (2013) 8895–8908.

[52] G. J. Long, P. J. Clarke, *Inorg. Chem.* 17 (1978) 1394–1401.

[53] D. B. G. Williams, M. Lawton, *J. Org. Chem.* 75 (2010) 8351–8354.

[54] *SAINT-Plus*, version 7.06a and APEX2; Bruker-Nonius AXS Inc.: Madison, WI, 2004.

[55] G. M. Shedrick, *Acta Crystallogr.* A64 (2008) 112–122.

[56] M. N. Burnett, G. K. Johnson. ORTEPIII. Report ORNL-6895. OAK Ridge National Laboratory; Tennessee, USA, 1996.

[57] (a) R. Supino, In Vitro Toxicity Testing Protocols, 1995, 137–149; (b) G. Rakić, S. Grgurić-Šipka, G. Kaluđerović, M. Bette, L. Filipović, S. Aranđelović, S. Radulović, Ž. Lj. Tešić, *Eur. J. Med. Chem*. 55 (2012) 214–219.

[58] P. Gans, A. Sabatini, A. Vacca, Talanta 43 (1996) 1739–1753.

[59] H. M. Irving, M. G. Miles, L. D. Pettit, *Anal. Chim. Acta* 38 (1967) 475–488.

[60] SCQuery, The IUPAC Stability Constants Database, Academic Software (Version 5.5).

[61] L. Zékány, I. Nagypál, in: Computational Methods for the Determination of Stability Constants, ed. D. Leggett, Plenum, New York, 1985.

[62] C. F. Baes, R. E. Mesmer, The Hydrolysis of Cations, Wiley, New York, 1976.

[63] E. Farkas, E. Kozma, T. Kiss, I. Toth, B. Kurzak, *J. Chem. Soc. Dalton Trans*. (1995) 477–481.

[64] V. B. Arion, M. A. Jakupec, M. Galanski, P. Unfried, B. K. Keppler, *J. Inorg. Biochem.* 91 (2002) 298–305.

[65] D. Carmona, M. P. Lamata, F. Viguri, I. Dobrinovich, F. L. Lahoz, L. A. Oro, *Adv. Synth. Catal*. 344 (2002) 499–502.

[66] (a) R. Noto, P. Lo Meo, M. Gruttadauria, G. Werber, *J. Heterocycl. Chem.* 36 (1999) 667–674; (b) S. Buscemi, M. Gruttadauria, *Tetrahedron* 56 (2000) 999–1004; (c) M. H. Shih, C. L. Wu, *Tetrahedron* 56 (2005) 0917–10925; (d) A. Foroumadi, S. Pournourmohammadi, F. Soltani, M. Asgharian-Rezaee, S. Dabiri, A. Kharazmi, A. Shafiee, *Bioorg. Med. Chem. Lett.* 15 (2005) 1983–1985; (e) A. Foroumadi, Z. Kiani, F. Soltani, *Farmaco* 58 (2003) 1073–1076; (f) J. P. Kilburn, J. Lau, R. C. F. Jones, *Tetrahedron Lett.* 44 (2003) 7825–7828; (g) R.

Severinsen, J. P. Kilburn, J. F. Lau, *Tetrahedron* 61 (2005) 5565–5575; (h) E. López-Torres, A. R. Cowley, J. R. Dilworth, *Dalton Trans.* (2007) 1194–1196.

[67] (a) J. S. Casas, M. V. Castaño, E. E. Castellano, M. S. García-Tasende, A. Sánchez, M. L. Sánchez, J. Sordo, *Eur. J. Inorg. Chem.* (2000) 83–89; (b) J. S. Casas, M. V. Castaño, M. S. García-Tasende, A. Sánchez, J. Sordo, A. Touceda, *Polyhedron* 24 (2005) 3057–3065; (c) J. S. Casas, M. V. Castaño, E. E. Castellano, J. Ellena, M. S. García-Tasende, A. Gato, A. Sánchez, L. M. Sanjuán, J. Sordo, *Inorg. Chem.* 41 (2002) 1550–1557; (d) A. Castiñeiras, I. García-Santos, S. Dehnen, P. Sevillano, *Polyhedron* 25 (2006) 3653–3660; (e) J. S. Casas, M. V. Castaño, M. S. García-Tasende, E. Rodríguez-Castellón, A. Sánchez, L. M. Sánchez, J. Sordo, *Dalton Trans.* (2004) 2019–2026.

[68] (a) S. K. Dutta, S. Samanta, D. Ghosh, R. J. Butcher, M. Chaudhury, *Inorg. Chem.* 41 (2002) 5555–5560; (b) Y. Deng, Y. Yang, Y. Zhang, Q. Yan, J. Liu, *J. Coord. Chem.* 65 (2012) 1409–1416; (c) M. Rubčić, D. Milić, G. Horvat, I. Đilović, N. Galić, V. Tomišić, M. Cindrić, *Dalton Trans.* (2009) 9914–9923.

[69] E. A. Enyedy, M. F. Primik, C. R. Kowol, V. B. Arion, T. Kiss, B. K. Keppler, *Dalton Trans.* 40 (2011) 5895–5905.

[70] J. Shao, B. Zhou, A.J. Di Bilio, L. Zhu, T. Wang, C.Q.J. Shih, Y. Yen, Mol. Cancer Ther. 5 (2006) 586–592.

[71] É. A. Enyedy, N. V. Nagy, É. Zsigó, C. R. Kowol, V. B. Arion, B. K. Keppler, T. Kiss, *Eur. J. Inorg. Chem.* (2010), 1717−1728.

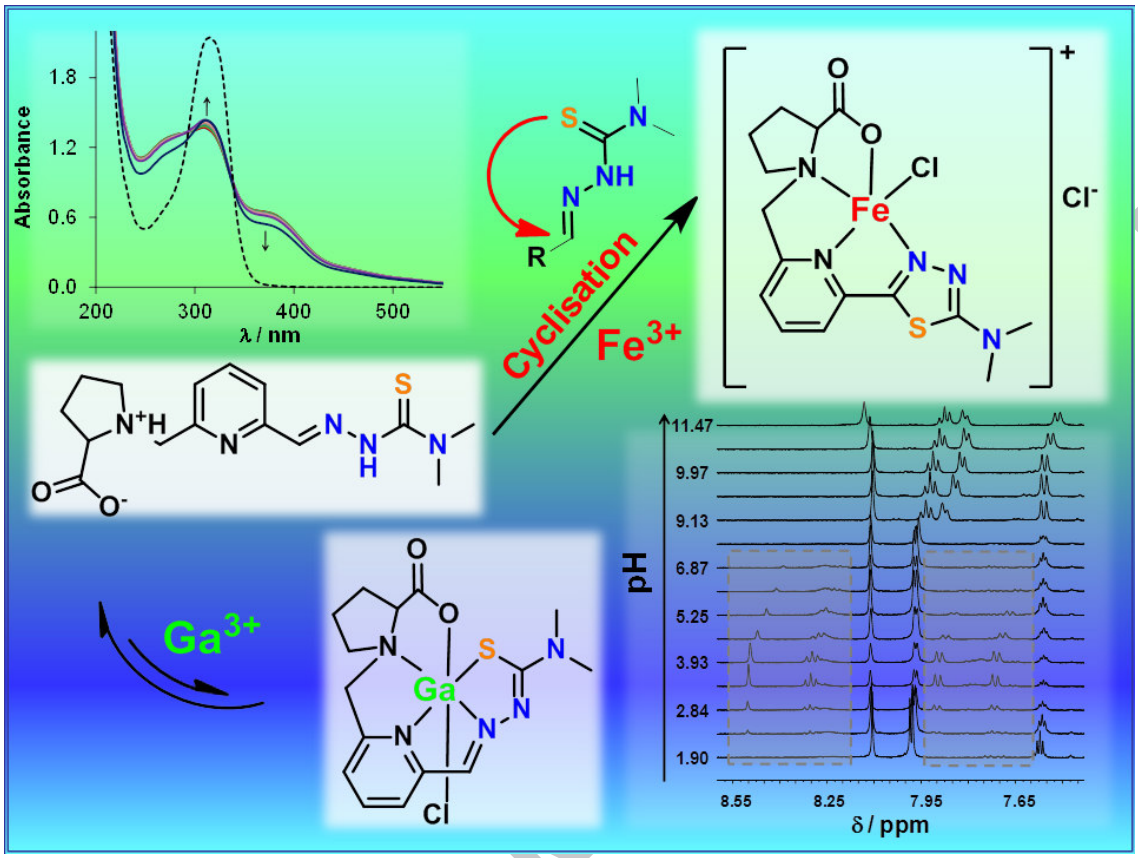

Synopsis

Two gallium(III) complexes with L-proline-thiosemicarbazone hybrids have been synthesised and comprehensively characterised. Reaction of iron(III) with the terminally dimethylated L-proline-thiosemicarbazone hybrid led to an oxidative cyclisation of the ligand and isolation of an iron(III) complex. The cytotoxicity of the new compounds was studied on three human cancer and one normal cell line, revealing no or low activity. The complexation reactions with iron(II), iron(III) and gallium(III) were studied in solution by using different methods. The low stability of the gallium(III) complexes at physiological pH and the low iron(II) binding affinity of the ligand precursors most probably contributes to the low antiproliferative activity of the studied substances.

Highlights

New gallium(III) and iron(III/II) complexes with L-proline-thiosemicarbazone hybrids were synthesised.

Comprehensive characterisation(1D/2D NMR, UV–vis, ESI MS and X-ray crystallography) of gallium(III) and iron(III) complexes.

In vitro antiproliferative activity was evaluated.

Solution stability of gallium(III) and iron(III/II) complexes investigated by pH-metry, ^{1}H NMR- and UV–vis spectroscopies.